Nucleation Induction Time in Levitated Droplets

Dragutin Knezic,[†] Julien Zaccaro,[‡] and Allan S. Myerson*,[†]

Illinois Institute of Technology, 3301 South Dearborn, Siegal Hall 103, Chicago, Illinois, and Laboratoire de Cristallographie CNRS, BP 166, 38042 Grenoble cedex 09, France

Received: January 29, 2004; In Final Form: May 3, 2004

Nucleation induction times of the protein lysozyme in aqueous solution were studied using electrodynamic levitation of single solution droplets. This technique allows the study of homogeneous nucleation by the elimination of dust, dirt, and container walls. A new experimental procedure was employed, which allowed control of the relative humidity around the supersaturated droplet and thus allowed the measurement of nucleation induction time at a given supersaturation. This measurement was performed 510 times at essentially identical conditions to obtain sufficient data to examine the statistics of nucleation induction time. An analysis of the data using the classic approach of Turnbull and a newly proposed two-step treatment is presented.

Introduction

Crystallization from solution is an important separation and purification process used in the chemical and pharmaceutical industries. Nucleation of a solute in a supersaturated solution is the first step of the phase separation process. Kashchiev[1] describes the nucleation as "the process of random generation of those nanoscopically small formations of the new phase that have the ability for irreversible overgrowth to macroscopic sizes". This randomness implies that nuclei are not formed immediately upon the achievement of supersaturation. The nucleation induction time is the period from the achievement of supersaturation to the formation of the new phase. The detection of the new phase is indicated by the appearance of crystals or by changes in some of the physical properties (e.g., turbidity and refractive index) of the solution. The induction time is the sum of the transient time that is needed to reach a steady state of nucleation, the nucleation time, and the time that is required for the critical nucleus to grow to a detectable size.[2] The transient period is unimportant in aqueous solutions of moderate supersaturations and viscosity.[3]

A comprehensive theory of the nucleation of crystalline solutes from solution does not exist at present, but there is growing evidence that it is a two step process: the formation of liquidlike clusters of solute molecules that is followed by the rate-limiting organization of such clusters into a protocrystal.[4] Garetz et al.[5] recently reported on the polarization switching of a glycine crystal structure by nonphotochemical light-induced nucleation. In this work, intense pulses of near-infrared light-induced nucleation of aged supersaturated glycine solutions and the polarization state of the light controlled the crystal form that was obtained. It is postulated that the electric field of the laser aids in the organization of the liquidlike clusters already present in the solution. This result is consistent with the observation that the nucleation of crystalline materials from solution becomes more difficult (longer induction times) as the complexity of molecules increases because it is more difficult for more complex molecules to arrange themselves in the appropriate lattice structure.

Protein molecules attach themselves to one another via specific binding sites to form aggregates that serve as nucleating sites for crystal growth. The probability of solute collisions increases with concentration, so supersaturated conditions enhance the chance of creating a critical-size nucleus. Higher supersaturation levels require a smaller minimal thermodynamically stable aggregate (critical nucleus) for the onset of nucleation. An increase in the supersaturation level enhances the probability of nucleation.[6] The metastable zone of protein solutions is much wider than those of small molecules[7] so that protein nucleation begins at very high levels of supersaturation, "often several hundred to thousand percent".[8] In this nonequilibrium state of high supersaturation, molecules continually combine to form clusters and dissociate back into solution. Once the critical size is reached, the aggregate starts to grow spontaneously.[9] McPherson et al.[8] hypothesize that in crystal nuclei molecules tend to interact in all three directions in a periodic manner whereas amorphous precipitates lean toward linear arrangements with arbitrary branching.

Nucleation-Induction Periods. Previous investigators measured the nucleation induction time of inorganic crystalline materials directly using a light-scattering method.[10,11] Other studies examined changes in properties, such as solute concentration,[12] conductivity changes in supersaturated solutions in the presence of additives,[13] and conductivity changes in inorganic reaction mixtures.[14] Lysozyme mixtures have been used in the determination of the induction time of lysozyme crystals by laser diffraction. Supersaturation was achieved through temperature variation. The results show that the induction period increases exponentially with decreasing supersaturation of the solution.[15] Drenth et al.[16] measured the induction time in lysozyme crystallization using NMR, taking into account the anisotropy of the interaction of protein molecules. The results indicated that small critical nuclei consist of a linear, fiberlike structure whereas larger ones have a more compact structure.

Lately, the findings of several investigators indicate that having a solution near a liquid−liquid (L−L) line is helpful in obtaining greater nucleation rates and slower crystal growth, which could result in well-defined crystals. Muschol and

* Corresponding author. Tel: (312) 567 3163. Fax: (312) 567 7018. E-mail: myerson@iit.edu.
[†] Illinois Institute of Technology.
[‡] Laboratoire de Cristallographie CNRS.

10.1021/jp049586s CCC: $27.50
Published on Web 06/22/2004

Rosenberger[17] found that cycling through the L−L two-phase region strongly enhances the rate of formation of crystals but is detrimental for obtaining large crystals of good quality. The induction time of the nucleation process is strongly reduced by the cycling procedure. Galkin and Vekilov[18] measured homogeneous nucleation rates at a constant temperature of 12.6 °C and varied the thermodynamic supersaturation by changing the concentrations of the protein and the precipitant. It was found that the existence of a second liquid phase at high protein concentrations strongly affects crystal nucleation kinetics in two ways: First, in the region of L−L demixing, the nucleation rate is lower than expected for a given temperature and protein concentration. Second, slightly above this phase boundary, experiments yielded nucleation rates that varied by a factor of up to 2 for the same experimental conditions. Galkin and Vekilov[19,20] show that the rate of homogeneous nucleation of lysozyme crystals passes through a maximum in the vicinity of the liquid−liquid phase boundary hidden below the liquidus (solubility) line in the phase diagram of the protein solution. Also found was that for the chosen model (lysozyme) crystal nucleation is an intrinsically stochastic process. In this respect, protein nucleation is similar to the nucleation of simple liquids or water-soluble inorganic materials.

Homogeneous Nucleation. Supersaturated solutions are in a nonequilibrium state. The overall concentration of the species at a given temperature is constant, but on a microscale, fluctuations induce ordered regions of clusters. Classical nucleation theory states that once the critical size of the cluster is formed crystallization takes place because the overall Gibbs free energy of the solution is lowered. The rate of nucleation (J) by this mechanism is

$$J = A \exp\left(\frac{-\Delta G_{cr}}{kT}\right) \tag{1}$$

where A is a preexponential factor and has a theoretical value of 10^{30} (nuclei/cm^3), T is the temperature, k is the Boltzman constant, and ΔG_{cr} is the critical free energy for nucleation. In the case of heterogeneous nucleation, impurities that lower the free-energy barrier are needed for the formation of a critical cluster[2]. Mullin[21] states that the amount of energy necessary to produce a stable nucleus can be expressed with eq 2

$$\Delta G_{cr} = \frac{16\pi\gamma^3 v^2}{3(kT \ln S)} \tag{2}$$

where γ is the interfacial tension of the solid in the solution, v is the molecular volume, and S is the supersaturation level.

The experimental investigation of nucleation (homogeneous or heterogeneous) is very complicated. This complexity arises from the small sizes of the critical nuclei, which makes it difficult to observe them directly and, consequently, to measure nucleation parameters. Another difficulty associated with nucleation studies is the contamination of the crystallizing phase. Nucleation proceeds more readily on the surfaces of the foreign objects (dust, microparticles, and container walls) present in the solution. In the absence of the impurities or bulk wall effects, homogeneous nucleation occurs. The probability of nucleating throughout the sample is identical, and the rate of nucleation depends on how readily the nucleus is formed within the sample. A number of investigators have attempted to measure induction time statistics. Because nucleation is believed to be a stochastic process, a statistical distribution of the induction times is very important.

The work of Turnbull[22] involved the investigation of homogeneous nucleation of liquid metals. The sample was dispersed into a large number of small droplets inside a nonoxidizing liquid matrix to prevent oxidation and exclude contact with solid walls. In this manner, the macroscopic impurities are contained in individual drops. Upon cooling, some drops crystallized before others at smaller supercoolings because of the presence of the impurities (heterogeneous nucleation). The majority of the drops underwent the greatest supercooling, and they were considered to crystallize as a result of homogeneous nucleation. Compared to heterogeneous nucleation, the maximum supercoolings of homogeneous nucleation are more reproducible because the impurities are eliminated. Chernov[23] states that the nucleus forms by accident and is a product of localized fluctuation. The probability of its occurrence within the time dt is JV dt, where V is the drop volume and J is the nucleation rate.

The fraction of drops not frozen at time t is, therefore, expressed by the relation

$$\frac{N}{N_0} = \exp(-JVt) \tag{3}$$

where N = the number of uncrystallized samples and N_0 = the total number of samples.

Barlow and Haymet[24] used an automated apparatus to study heterogeneous nucleation by repeatedly freezing (350 times) a sample of supercooled liquid (water + insoluble AgI crystals) at constant freezing temperature. Performing many independent experiments (N_0) on the same sample is equivalent to performing a single experiment on N_0 perfect replicas of the same sample. The assumption was made that the sample does not change with time and is not affected by any changes resulting from temperature cycling or aging with time. It was determined that the mechanism of nucleation follows a stochastic process obeying first-order kinetics.

Because nucleation is a stochastic phenomenon, Izmailov et al.[25] suggested using a linear quadrupole electrodynamic levitator trap (LQELT) to gather a large enough set of experimental data for nucleation statistics. This technique would allow the simultaneous containerless suspension of $N = 150-300$ electrically charged microdroplets of supersaturated solution in the solvent atmosphere. Few such studies have been performed to obtain nucleation statistics. Kramer et al.[26,27] used an electrodynamic levitation trap with temperature control to study the homogeneous ice nucleation rates as a function of the droplet's temperature and charge. Shaw and Lamb[28] used an electrodynamic levitation cell to freeze water drops. The evaporation of a droplet as a function of time was included in their derivation of the droplet freezing probability. The homogeneous freezing rates determined by their measurements were consistent compared to those of other techniques. Weidinger et al.[29] distinguished homogeneous from heterogeneous nucleation by measuring the nucleation rates of the *n*-alkanes in an electrodynamic balance.

It is the purpose of this work to employ electrodynamic levitation to examine the nucleation of crystalline lysozyme from solution and to perform enough identical experiments to obtain nucleation induction time statistics.

Experimental Section

Electrodynamic Levitation Trap (ELT). Figure 1 shows the schematic representation of the SVELT apparatus.[30−32] The levitation trap provides a clean and simple environment for

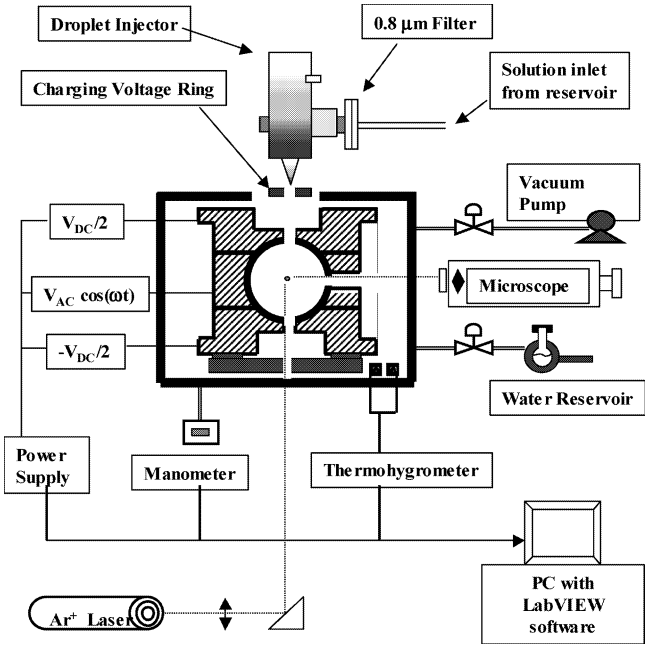

Figure 1. Schematic representation of the SVELT apparatus.

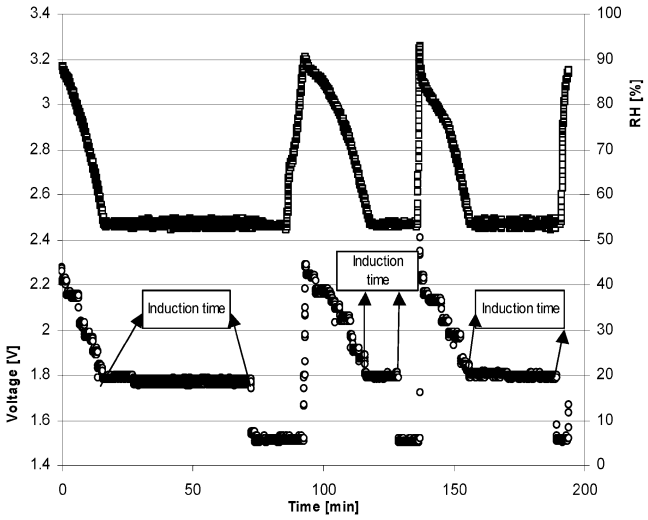

Figure 2. Experimental data for nucleation induction time: relative humidity vs time (upper plot) and voltage vs time (lower plot). The induction time was taken as the elapsed time between the creation of supersaturation (reaching the target relative humidity) and the detection of nucleation.

crystal formation. The SVELT configuration allows for the suspension of a single charged microdroplet inside an electrical field. Prior to injection into the trap, the solution is filtered through a 0.8-μm Millipore filter unit (Millex-PF) to remove any contamination. A piezoelectric droplet generator filled with the prefiltered solution forms the droplets of the solution to be analyzed. The diameter of the orifice in the glass tip of the droplet generator is approximately 120 μm, which allows the creation of the droplets to be 40−50 μm in diameter. Prior to the entrance of the trap, the drop passes through a charging ring (V_{dc} applied to the charging ring = 86−92) and as a result gets surface charged. The spherical internal configuration provides a symmetrical distribution of electrical potential inside the trap with the center of the trap experiencing zero ac field. The trap consists of three electrodes with isolation placed between each electrode. The middle electrode provides a moderate ac voltage (350−400 V) that oscillates the particle vertically along the axis of the trap, which is at the geometric center of the device. In addition to trapping the droplet in the electrodynamic levitation system, its weight must also be balanced out against the gravitational pull.

The top and bottom electrodes supply a dc voltage to counteract the pull of gravity and to stabilize and prevent the droplet from drifting from the trap. Both trapping and levitation are independently achieved in the ELT. The droplets can be suspended in this system for long periods of time and can be localized to a fraction of their diameter. The trap sits inside a stainless steel chamber and is isolated from its surroundings. This technique allows the examination of a single charged drop suspended in midair. A charged drop is captured inside an alternating electric field, and an opposing dc field compensates its gravitational pull. A particle will remain at rest at the center of the trap as along as the force due to the dc field exactly balances the gravitational force on the particle. The levitation technique allows the examination of homogeneous nucleation because there is no contact with the container walls. While the droplet is suspended in midair, the solvent is slowly evaporated. This method allows the creation of higher supersaturation conditions than in bulk solutions. In bulk solutions, the energy barrier for nucleation is lowered by the presence of foreign substances or container walls, which act as nucleating centers.

Experimental Conditions and Procedure for Nucleation Induction Time Measurements. The induction time measurements were performed on supersaturated droplets of aqueous protein solutions. The initial solution condition for a nucleation induction experiments was 4% wt [($m_{solute}/m_{solution}$) × 100] chicken egg white lysozyme (L-6876, lot 65H7025, 3× crystallized, dialyzed, and lyophilized, approximately 95% protein) to 1% [($m_{solute}/m_{solution}$) × 100] sodium chloride in 0.1 M sodium acetate buffer of pH 4.0. This solution was placed in the reservoir and fed to the droplet generator. Four drops of approximately the same final voltage (mass) were used for the experiments. It was assumed that the same amount of solid would deliquesce in the same manner, producing droplets very similar in volume.

To measure the nucleation induction time, one has to create and maintain constant supersaturation in the droplet. Lowering the relative humidity inside the experimental chamber and maintaining it at a constant level achieves this requirement. An example of the experimental data for a few experiments of the same drop (relative humidity vs time and voltage vs time) can be seen in Figure 2. Once crystallization occurs, water vapor is slowly bled into a trap until the point of deliquescence. At that point, the water vapor stream is closed, and evacuating begins until a desired level of relative humidity is achieved. The induction time was taken to be the elapsed time between the creation of supersaturation (reaching the target relative humidity) and the detection of nucleation. It is assumed that a single nucleation event occurs, followed by very rapid crystal growth due to the high supersaturation present in the droplet. Visual observation through the microscope indicates the existence of a single lysozyme crystal. Experiments have been conducted with small-molecule systems in which single crystals formed by the nucleation of these droplets have been recovered.

The pressure of the chamber, the dc voltage, the relative humidity, and the time required for nucleation were recorded. The temperature of the chamber was monitored and recorded. About half of the experiments were discarded either because the drop crystallized before the desired target humidity was reached or because the temperature fluctuation during an experiment was too large. All of the experiments taken for analysis were performed at temperatures between 24.7−25.8 °C. Table 1 lists the number of experiments taken for analysis,

TABLE 1: Number of Experiments between 24.7 and 25.8 °C Used for Analysis[a]

drop	runs $T = 24.7-25.8$ °C	average V_{dc} just before crystallization	average V_{dc}^{dry}	average V_{dc}^{del}	w_p	w_p/w_p*
1	285	1.818	1.55	2.36	0.454	1285.37
2	7	1.815	1.6	2.36	0.469	1329.026
3	48	2.71	2.2	3.64	0.432	1223.893
4	170	2.45	2.02	3.4	0.439	1243.012
	510	**2.20**	**1.84**	**2.94**	**0.448**	**1270.325**

[a] The average dc voltage for the deliquescent point, crystallization point, voltage prior to crystallization, concentration of protein just before crystallization, and supersaturation expressed as the mass fraction ratio; w is the mass fraction of protein.

TABLE 2: Average Relative Humidity at the Deliquescent Point, Average Relative Humidity at the Crystallization Point, Average Transition Time from Deliquescence to Target Relative Humidity, and Ranges for These Averages[a]

drop	average RH^{del}	range	average $RH^{crystal}$	range	average transition time (min)	range
1	90.4	80.8−96	52.52	49.0−54.0	15.36	9.62−28.42
2	84.71	82−89	50.8	48.8−52.0	16.28	9.90−20.60
3	80.47	77−85	50.1	48.7−51.5	17	9.70−25.87
4	81.82	77−89	51	49.0−54.0	18.25	9.27−33.55

[a] RH is the relative humidity (%).

the average dc voltage for the deliquescent point, the average DC voltage for the crystallization point, the voltage prior to crystallization, the average mass fraction of protein just before crystallization occurred, and the average supersaturation before crystallization. Supersaturation was calculated as a ratio of the mass fraction of protein to the mass fraction of protein at saturation.

The solubility of the lysozyme at 0.1 M NaAc, pH 4.0, and 11.2% NaCl was measured by UV spectroscopy using the absorbance at 281 nm. The value obtained was 0.0353 g/100 mL. Table 2 lists the average relative humidity at the deliquescent point, the average crystallization point, and the average transition time from deliquescence to target relative humidity. Also included are the ranges for these averages.

Calculations Involving Induction Time Experiments. To calculate the volume of the droplet, we used eq 4:

$$\upsilon = \frac{m}{\rho} \tag{4}$$

where υ is the volume of the drop (cm^3), m is the mass of the drop (g), and ρ is the density of the drop (g/cm^3). The mass of the drop was determined by

$$m = Cq\frac{V_{dc}}{2z_0 g} \tag{5}$$

where m is the mass of the particle, g is the standard gravitational acceleration (9.81 m/s^2), q is the surface charge on the particle ($\sim 10^4-10^5$ e), z_0 is the characteristic length of the cell (for SVELT it is the radius of the spherical void ~0.5 cm), V_{dc} is the dc voltage applied, and C is a geometric constant ($C = 1$ for spherical void).

The value for V_{dc} was taken to be an average value of the voltage just before the crystallization for all drops. The average voltage calculated was 2.2 V. The mass of the droplet (for $q = 10^5$) was calculated to be 3.593×10^{-10} g. The density of the solution droplet prior to crystallization was determined by a densitometer with the assumption that the density increases linearly with the protein concentration. The densities of the buffer and the saturated solution were measured, and the density of the drop was calculated from the calibration curve for the protein concentration just before crystallization occurred. This density (1.125 g/cm^3) was used to calculate the average volume of the droplet (2.25×10^{-10} cm^3).

TABLE 3: Coefficients for the Plots in Figure 3

	exponential	std error	Turnbull	std error	two step	std error
y_0	−0.4525	0.0183				
A	−0.0842	0.0013	−0.1000	0.0017	−0.4198	0.0109
α					0.5988	0.0079
R^2	0.8916		0.7574		0.9380	

Results and Discussion

The experiments showed a distribution of the nucleation induction times, and the nucleation of the droplets appears to be a random process, in agreement with the conclusions of Chernov[23] and Barlow and Haymet.[24]

The experimental data was plotted as the log of the ratio of uncrystallized to crystallized samples (N/N_0) versus the nucleation induction time and is presented in Figure 3. The parameters for all nucleation kinetic models examined were obtained by nonlinear regression analysis (Sigmaplot 2001) of the experimental data. The analysis of the simple exponential decay function results in a line, which unrealistically intersects the y axis at a value less than zero (green line in Figure 3). Following Turnbull's model for nucleation in liquid metals, we estimated parameters for eq 3; the model prediction is presented in Figure 3 (brown line). Table 3 presents the estimated values and the errors of the coefficients for the models. The rate of nucleation at supersaturation of $S = \ln(w/w_p) = 7.15$ (w is the mass fraction), was calculated to be 2.7×10^{10} nuclei/cm^3 s. Dixit et al.[33] compared the experimental estimates and model predictions of protein crystal nucleation rates. Large discrepancies occur at seemingly identical conditions for three different experimental methods. For example, at 3% NaCl, 0.05 M NaAc buffer, pH 4.5, $T = 13$ °C, and supersaturation defined in terms of ratio of volume fractions of solute $[\ln(\phi/\phi_s)] = 2.75$, the nucleation rates varied from 1 to 10^9 to 10^{14} nuclei/cm^3 s. Dixit et al.[33] developed a kinetic model for the prediction of nucleation rates and reported the nucleation rate of 10^{20} nuclei/cm^3 s. They speculate that the failure of these models lies in the approximate descriptions of the interaction potentials between protein molecules and the processes of aggregation and dissociation of single molecules on cluster surfaces that lead to crystal nucleation. The analysis based on Turnbull's approach (eq 3) for liquid metals does not correlate well with the data obtained for aqueous protein solutions. Because of the poor correlation, the nucleation rate calculated should be considered to be only an estimate.

Two-Step Nucleation Model. Turnbull's analysis applied to crystallization from a melt follows the classical nucleation theory, where the condition requirement for the precipitation is fulfilled once the cluster of the molecules reaches the critical size. Because Turnbull's approach does not appear to provide good correlation with the experimental data obtained for lysozyme nucleation, a new approach involving two random processes has been evaluated. In this approach, the fluctuation in concentration occurs randomly in the droplet, and as a result, clusters of molecules aggregate. Nucleation occurs when a critical size cluster of protein molecules forms and rearranges itself into the crystalline nucleus. The formation of one stable

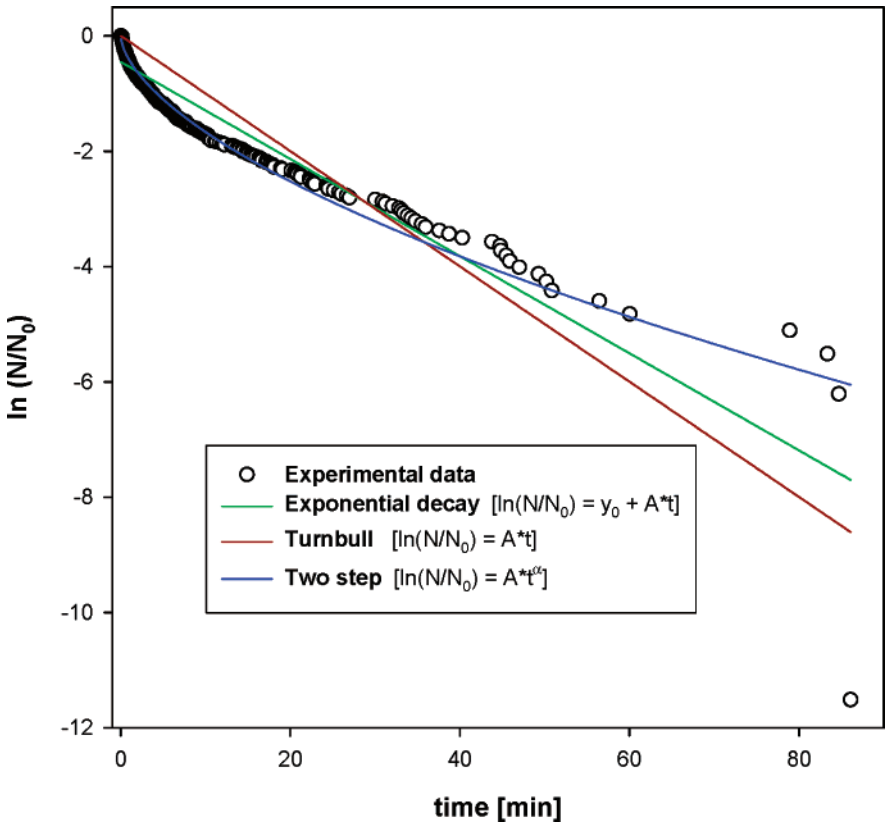

Figure 3. Plots of the logarithm of the ratio of uncrystallized to crystallized samples vs nucleation induction time. The two-step model (blue line) depicts the experimental data much better than the exponential decay function (green line) and the model based on Turnbull's analysis (brown line).

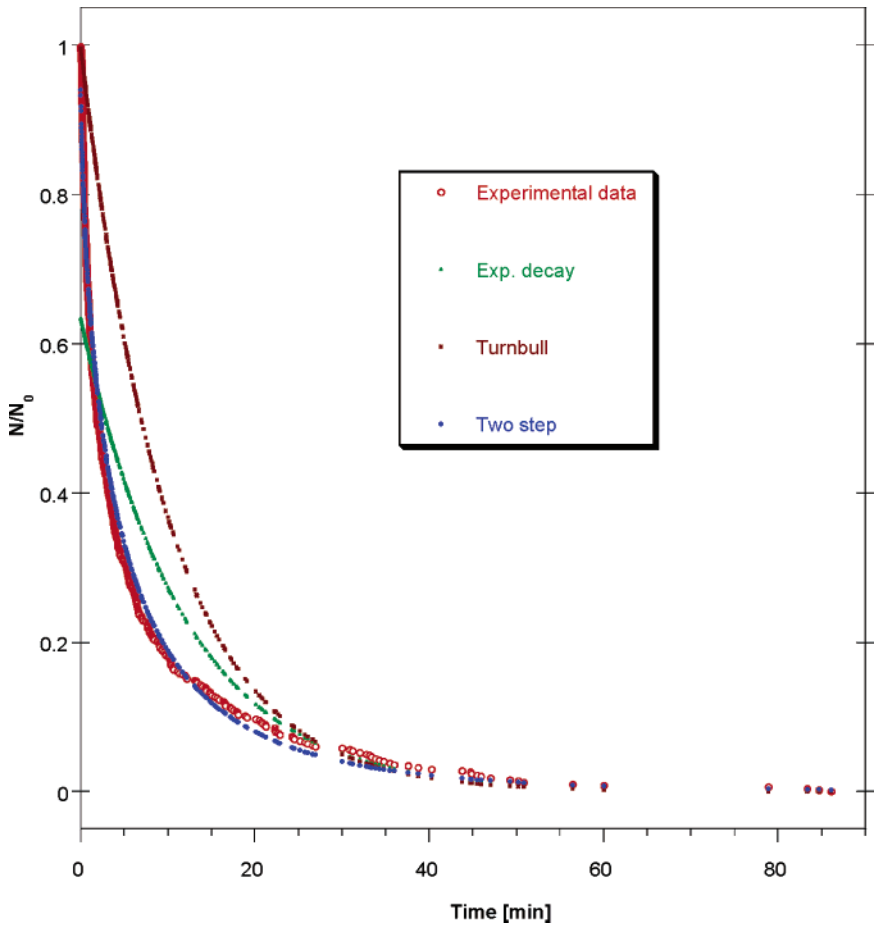

Figure 4. Fraction of uncrystallized droplets vs induction time: experimental data (red), exponential decay function (green), Turnbull's analysis (brown), and two-step model (blue).

crystalline nucleus will result in the nucleation of the entire drop. There are two random processes that occur inside a drop. The first is the fluctuation of the size of the clusters in the drop and is a function of supersaturation level with a Gaussian distribution. The second is the time taken for the clusters to rearrange themselves into a crystalline nucleus. The time required for this process is also randomly distributed. Usually these times are looked upon as being the same and are taken as zero. This condition corresponds to having $\alpha = 1$, where the second random process happens very fast and Turnbull's analysis can be applied. If the distribution can be described by a Poisson distribution, then the induction time can be explained by regular diffusion theory.

For other distributions, eq 6 is used:

$$\frac{N}{N_0} = \exp(-At^{\alpha}) \Rightarrow \ln\left(\frac{N}{N_0}\right) = -At^{\alpha} \qquad (6)$$

In Figure 3, the plot of the log of the ratio of uncrystallized drops versus nucleation induction time was fit with the two-step model (blue line). Table 3 presents estimated values of the coefficients for the two-step model (eq 6). The value of α deviates greatly from unity, indicating that the second random process does not happen instantaneously. This implies that the bulky protein molecules require some degree of orientation prior to forming a stable nucleus capable of further growth. It is expected that solutions containing smaller molecules (e.g., inorganic salts) will show α values close to 1. Preliminary experiments with ammonium sulfate nucleated from water confirm this to be the case. The ratio of N/N_0 versus induction time (where N/N_0 was calculated for each model from the coefficients that were extracted from the plots presented in Figure 3) is shown in Figure 4. The two-step model describes the behavior of the experimental data better than the analysis based on Turnbull's model.

Conclusions

The SVELT apparatus that we used for levitating droplets is an effective method for achieving constant levels of high supersaturation in the protein solutions and obtaining nucleation induction time statistics. The induction time for the lysozyme droplets was random, and the nucleation rate calculated on the basis of Turnbull's analysis was 2.7×10^{10} nuclei/cm^3 s. The experimental data showed significant deviation from Turnbull's model and was better described by the two-step model.

Data for additional systems such as simple inorganic salts and organic molecular crystals of low molecular weight is currently being collected to determine the relationship between molecular complexity and the power α in the two-step model. Preliminary data on the ammonium sulfate−water system indicates the postulated value of 1 for systems in which the molecular rearrangement step is rapid.

Acknowledgment. Grateful acknowledgment is given to Dr. Alexander Izmailov for lengthy discussions on the theoretical developments of two-step model and to Dr. Stephen Arnold for many helpful discussions regarding SVELT operation. This work was supported by NASA (grant no. NAG8-1370).

References and Notes

(1) Kashchiev, D. *Nucleation: Basic Theory with Applications*; Butterworth-Heinemann: Boston, MA, 2000.
(2) Myerson, A. S. *Handbook of Industrial Crystallization*, 2nd ed.; Butterworth-Heinemann: Boston, MA, 2002.
(3) Sohnel, O.; Mullin, J. W. *J. Colloid Interface Sci.* **1988**, *123*, 43.
(4) Shore, J. D.; Perchak, D.; Shnidman, Y. *J. Chem. Phys.* **2000**, *113*, 6276.
(5) Garetz, B. A.; Matic, J.; Myerson, A. S. *Phys. Rev. Lett.* **2002**, *89*, 175501.
(6) Rosenberger, F.; Muschol, M.; Thomas, B. R.; Vekilov, P. G. *J. Cryst. Growth* **1996**, *168*, 1.
(7) Pusey, M. L. *J. Cryst. Growth* **1991**, *110*, 60.
(8) McPherson, A.; Malkin, A. J.; Kuznetsov, Y. G. *Structure* **1995**, *3*, 759.
(9) Kam, Z.; Shore, H. B.; Feher, G. *J. Mol. Biol.* **1978**, *123*, 539.
(10) Wojciechowski, K.; Kibalczyc, W. *J. Cryst. Growth* **1986**, *76*, 379.
(11) Fawell, P. D.; Watling, H. R. *Appl. Spectrosc.* **1998**, *52*, 1115.
(12) Skrtic, D.; Markovic, M.; Komunjer, Lj.; Furedi-Milhofer, H. *J. Cryst. Growth* **1984**, *66*, 431.
(13) Van Der Leeden, M. C. *J. Colloid Interface Sci.* **1992**, *152*, 338.
(14) Sohnel, O.; Mullin, J. W. *J. Cryst. Growth* **1978**, *44*, 377.
(15) Biscan, B.; Laguerie, C. *J. Phys. D: Appl. Phys.* **1993**, *26*, B113.
(16) Drenth J.; Dijkstra K.; Haas C.; Leppert J.; Ohlenschläger O. *J. Phys. Chem. B* **2003**, *107*, 4203.
(17) Muschol, M.; Rosenberger, F. *J. Chem. Phys.* **1997**, *107*, 1953.
(18) Galkin, O.; Vekilov, P. G. *J. Am. Chem. Soc.* **2000**, *122*, 156**.**
(19) Galkin, O.; Vekilov, P. G. *Chemistry* **2000**, *97*, 6277.
(20) Galkin, O.; Vekilov, P. G. *J. Cryst. Growth* **2001**, *232*, 63.
(21) Mullin, J. W. *Crystallization*, 4th ed.; Butterworth-Heinemann: Woburn, MA, 2001.
(22) Turnbull, D. *J. Chem. Phys.* **1952**, *20*, 411.
(23) Chernov, A. A. *Modern Crystallography III*; Springer-Verlag: New York, 1984.
(24) Barlow, T. W.; Haymet, A. D. J. *Rev. Sci. Instrum.* **1995**, *66*, 2996.
(25) Izmailov, A. F.; Myerson, A. S.; Arnold, S. *J. Cryst. Growth* **1999**, *196*, 234.
(26) Kramer, B.; Schwell, M.; Hubner, O.; Vortisch, H.; Leisner, T.; Ruhl, E.; Baumgartel, H.; Woste, L. *Ber. Bunsen-Ges. Phys. Chem.* **1996**, *100*, 1911.
(27) Kramer, B.; Schwell, M.; Hubner, O.; Vortisch, H.; Leisner, T.; Ruhl, E.; Baumgartel, H.; Woste, L. *J. Chem. Phys.* **1999**, *111*, 6521.
(28) Shaw, R. A.; Lamb, D. *Geophys. Res. Lett.* **1999**, *26*, 1181.
(29) Weidinger, I.; Klein, J.; Stockel, P.; Baumgartel, H.; Leisner, T. *J. Phys. Chem. B* **2003**, *107*, 3636.
(30) Arnold, S.; Hessel, N. B. *Rev. Sci. Instrum.* **1985**, *56*, 2066.
(31) Arnold, S.; Folan, L. M. *Rev. Sci. Instrum.* **1987**, *58*, 1732.
(32) Arnold, S. *Rev. Sci. Instrum.* **1991**, *62*, 3025.
(33) Dixit N. M.; Kulkarni, A. M.; Zukoski, C. F. *Colloids Surf., A* **2001**, *190*, 47.